Multi-agent technology based voltage grading control method for distribution network

Guangmao Liu[1], *Jiangtao* Chen[2] , *Runrun* Li[2] , *Jialin* Jin[2] , and *Yuying* Cheng[3,*]

[1]State Grid Sanmenxia Electric Power Supply Company, 472000 Sanmenxia, Henan, China
[2]State Grid Lushi County Electric Power Supply Company, 472200 Lushi, Sanmenxia, Henan, China
[3]Wuhan University of Technology, School of Mechanical and Electronic Engineering, 430070 Wuhan, Hubei, China

Abstract. It is one of the challenges to solve the power quality problems such as voltage fluctuation and voltage exceeding limit caused by the large-scale grid connection of distributed photovoltaic (DPV). Considering the operation speed of voltage regulation control in distribution network, this paper proposes a voltage hierarchical control method based on multi-agent structure. The mathematical models of this method are divided into dual-time scale global optimization model and event-triggered voltage regional autonomy model, aiming at solving the problem of operation safety of voltage exceeding limit. The method is verified by a specific example. The results show that this method can respond quickly to the change of power grid voltage, and help to reduce the risk of voltage exceeding the limit, and improve the operation economy of distribution network.

1 Introduction

Photovoltaic (PV) power generation has many advantages such as environmental friendliness and no noise pollution. In recent years, with the large-scale interconnection of distributed photovoltaic (DPV), a series of power quality problems have been caused, which makes the operation safety of distribution network decline. At the same time, DPV power generation as voltage regulating equipment also increases the complexity of voltage regulation control in distribution network.

Different from the traditional mathematical optimization method based on power flow optimization in voltage hierarchical control, multiple agent system (MAS) uses agent-based rule derivation and knowledge processing system to build an optimization model, and uses the autonomy and cooperation ability of agents to achieve the optimization goal of complex systems. Its physical structure is generally composed of three levels: distribution network agent, regional agent and unit agent.

The broadcast centralized communication method is adopted between regional agent and unit agent in centralized communication mode, which has the following problems:

* Corresponding author: chengyuying@whut.edu.cn

1) In the distribution network with high-permeability photovoltaic, the active and reactive power flows of the system change dramatically and influence each other, which increases the control complexity;

2) The regional agent needs to perform multiple regional power flow calculations to limit its operation speed.

Reference [1] based on the consistency theory, the reactive power compensation and active power reduction of voltage regulation are allocated according to the inverter capacity ratio. Reference [2] calculates the active-voltage sensitivity coefficient between photovoltaic node and overvoltage node through power flow calculation, and shares the active reduction according to the ratio of the coefficients. Reference [3] proposes that the distribution network should be divided into active and reactive power decoupling zones, and the output adjustment strategies based on the best sensitivity should be formulated within the active and reactive power zones respectively, so as to achieve the goal of maximizing the reactive power adjustment capability of inverters first and then minimizing photovoltaic active power cutting, but regional power flow calculation should be carried out after each output adjustment in the control process. Reference [4] aims at ensuring the voltage quality of the system and maximizing the active output of DPV, and proposes a distributed control strategy consisting of local prevention, distributed control in emergency and power recovery control. During the control process, DPV units only communicate with neighboring units. Based on this communication scheme, reference [5] designed a DPV output adjustment strategy of reactive power compensation first, and then evenly reducing the active power. When the voltage is out of limit after all reactive power capacity in the system is put into operation, the active power of DPV will be evenly reduced.

To solve the above problems, this paper introduces distributed control logic to design regional voltage control strategy, and obtains a real-time model of over-limit voltage based on event triggering. Detailed mathematical models and design solutions are designed for each control level. Finally, the PG-E69 bus system verifies the effectiveness of the proposed control method.

2 Architecture of voltage grading control

2.1 MAS

By using the autonomy and cooperation ability of agent, MAS can give consideration to the coordination of local and whole-network objectives of the system, and realize the multi-objective optimization of system economy, security and cleanliness. In the three-level voltage control architecture of distribution network, MAS has obvious advantages in response speed compared with traditional centralized control method for hierarchical voltage control in short time scale. Using multi-agent technology to realize voltage hierarchical control of distribution network can make up for the difference between global optimization and local control in time scale and space scale, and realize a voltage control scheme that takes into account the complexity of distribution network and real-time dispatching.

2.2 Control framework

The voltage classification control flow proposed in this paper is shown in Fig. 1. Among them, the two control levels, voltage and reactive power planning and short-term optimization of active and reactive power coordination, adopt the global voltage optimization model and solve it in the distribution network agent. The over-voltage real-time control level adopts the

regional voltage optimization model, which is solved by the unit-level agent through mutual communication and built-in solver.

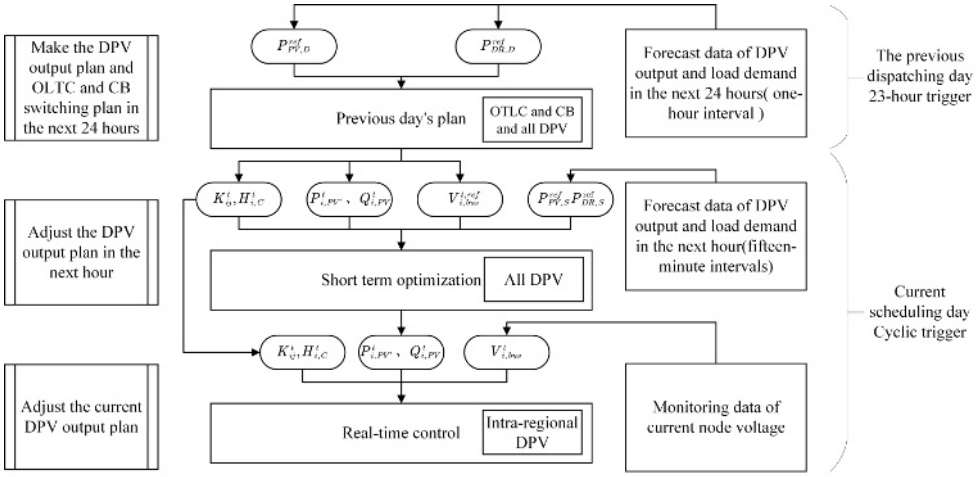

Fig. 1. Voltage classification control flow chart.

3 Establishment of optimization model

3.1 Previous day's plan of voltage reactive power

The previous day's plan of voltage reactive power can get the forecasting curve of DPV output and system load demand in the next 24 hours. The optimization goal of it is to reduce the network loss cost, reduce the power purchase cost of the system, and reduce the operation times of traditional voltage regulating equipment SVC and OLTC. The plan will make the action plan of OLTC, CB and other discrete voltage regulating equipment in the next day. The objective function of the model is:

$$\min F_{op} = F_{loss} + F_{switch} + F_{buy} \tag{1}$$

Where: F_{op} is the total cost in a complete operation cycle, and F_{loss} is the network loss cost of the system, F_{switch} is the voltage regulation cost of discrete equipment, including OLTC gear adjustment cost and CB switching cost, and F_{buy} is the cost of the system to purchase electricity from the superior power grid.

The model constraints include system power flow constraints and equipment operation constraints. The power flow constraints include node power flow constraints, branch power flow constraints, node voltage security constraints, branch current carrying capacity constraints, gateway power balance constraints and node power constraints. Equipment operation constraints include adjustment capability constraints of OLTC, CB and DPV.

(1) System power flow constraints

The power flow constraints of node *j* are:

$$\begin{cases} \sum_{i\in u(j)} \left(P_{ij}^t - r_{ij}\cdot\right) + P_j^t \cdot \left(I_{ij}^t\right)^2 = \sum_{k\in v(j)} P_{jk}^t \\ \sum_{i\in u(j)} \left(Q_{ij}^t - x_{ij}\cdot\left(I_{ij}^t\right)^2\right) + Q_j^t = \sum_{k\in v(j)} Q_{jk}^t \end{cases} \tag{2}$$

$$\left(I_{ij}^{t}\right)^{2}=\frac{\left(P_{ij}^{t}\right)^{2}+\left(Q_{ij}^{t}\right)^{2}}{\left(U_{i}^{t}\right)^{2}} \tag{3}$$

The power flow constraint of branch *ij* is:

$$\left(U_{i}^{t}\right)^{2}-\left(U_{j}^{t}\right)^{2}=2\left(r_{ij}\cdot P_{ij}^{t}+x_{ij}\cdot Q_{ij}^{t}\right)-\left(r_{ij}^{2}+x_{ij}^{2}\right)\cdot\frac{\left(P_{ij}^{t}\right)^{2}+\left(Q_{ij}^{t}\right)^{2}}{\left(U_{i}^{t}\right)^{2}} \tag{4}$$

where, $u(j)$ and $v(j)$ respectively represent the other end of the branch with node *j* as the end node and the initial node. $r_{i\,j}$ and $x_{i\,j}$ are the line resistance and reactance of branch *ij* respectively. U_i^t and $U_j^t$are the voltage amplitudes at node *i* and node *j* at time t respectively. P_i^t and Q_j^tpoints are the active power and reactive power at node *j* at time *t*, respectively, with injection into power grid as the positive direction. P_{ij}^t and $Q_{ij}^t$are respectively the active and reactive power flows at branch *ij* at time *t*, with node *i* flowing to node *j* as the positive direction.

The voltage safety constraint of nodes is:

$$U_{i}^{\min}\le U_{i}^{t}\le U_{i}^{\max} \tag{5}$$

The branch current safety constraint is:

$$I_{ij}^{t}\le I_{ij}^{\max} \tag{6}$$

The gateway power balance constraint is:

$$P_{0}^{\min}\le P_{0}^{t}\le P_{0}^{\max} \tag{7}$$

The node power balance constraints are:

$$\begin{cases}P_{j}^{t}=P_{j,PV}^{t}-P_{j,\text{load}}^{t}\\ Q_{j}^{t}=Q_{j,PV}^{t}+Q_{j,CB}^{t}-Q_{j,\text{load}}^{t}\end{cases} \tag{8}$$

In equations (2) to (8), P_0^{max} and P_0^{min} are the upper and lower limits of the active power interaction between the system and the superior power grid respectively, which are used to prevent the system regulation and control process from causing great influence on the superior power grid. U_i^{max} and U_i^{min} are the upper and lower limit values of the voltage amplitude of the system node respectively. I_{ij}^{max} is the upper limit of current at branch *ij*. $P_{j,PV}^t$ and $Q_{j,PV}^t$ are the actual active power and reactive power of DPV at node *j* at time *t*, respectively. $P_{j,load}^t$ and $Q_{j,load}^t$ are the actual active power and reactive power of the load at node *j* at time *t* respectively. $Q_{j,CB}^t$ is the actual reactive power of CB at node *j* at time *t*. When the above equipment is not incorporated at node *j*, the value of the corresponding power term is 0.

(2) Equipment operation constraints

1)OLTC operation constraints

In the actual operation of the system, in order to avoid frequent adjustment of OLTC, the upper limit of action times in the whole operation cycle must be constrained, and the adjustment of OLTC gear is a discrete action, and its operation constraints are:

$$\begin{cases} K_{ij}^{t} = K_{ij}^{\min} + M_{ij}^{t} \cdot K_{ij}^{step} \\ K_{ij}^{step} = \left(K_{ij}^{\max} - K_{ij}^{\min}\right) \Big/ M_{ij}^{\max} \\ M_{ij}^{\min} \le M_{ij}^{t} \le M_{ij}^{\max} \\ \sum_{t=1}^{T-1} \left| M_{ij,t+1} - M_{ij,t} \right| \le M_{ij}^{OLTC\lim} \end{cases} \tag{9}$$

where, K_{ij}^{max} and K_{ij}^{min} are the upper and lower limits of the transformer at branch ij respectively; M_{ij}^{max} and M_{ij}^{min} are the upper and lower limits of the gear of the transformer at branch ij respectively; K_{ij}^{step} is the ratio adjustment step; K_{ij}^{t} is the actual variable ratio of transformer at branch ij at time t; $M_{j}^{OLTClim}$ is the upper limit of gear adjustment times in one operation cycle; M_{ij}^{t} is the actual gear of the transformer at branch ij at time t.

2)CB operation constraints

In order to avoid frequent switching of CB, the upper limit of action times in the whole operation cycle must be constrained, and the switching of CB gear is a discrete action, similar to OLTC operation constraint, which is:

$$\begin{cases} H_{i,C}^{\min} \le H_{i,C}^{t} \le H_{i,C}^{\max} \\ Q_{i,C}^{t} = Q_{i,C}^{\min} + H_{i,C}^{t} \cdot Q_{i,C}^{\text{step}} \\ H_{i,C}^{t} \in \{Z\} \\ \sum_{t=1}^{T-1} \left| H_{i,C}^{t+1} - H_{i,C}^{t} \right| \le H_{i,C}^{\lim} \end{cases} \tag{10}$$

where, $H_{i,C}^{max}$ and $H_{i,C}^{min}$ are the upper and lower limits of CB gear at system node *i* respectively; $Q_{i,C}^{min}$ is the reactive power value accessed by CB at node *i* under the minimum gear; $H_{i,C}^{lim}$ is the upper limit of switching times of CB gear at node *i* in the whole operation cycle; $Q_{i,C}^{step}$ adjust step size for CB reactive power at node *i*; $H_{i,C}^{t}$ is the actual gear at node *i* at time *t*, which is a non-negative integer.

3) DPV operation constraints

At the planned control level, all active power generation of DPV is connected to the grid, and its operation constraint expression is as follows:

$$\begin{cases} 0 \le P_{j,PV}^{t} \le P_{j,t,PV}^{pre} \\ \left(P_{j,PV}^{t}\right)^2 + \left(Q_{j,PV}^{t}\right)^2 \le \left(S_{j,PV}^{\max}\right)^2 \\ -Q_{j,t,PV}^{pre} \le Q_{j,PV}^{t} \le Q_{j,t,PV}^{pre}, Q_{j,t,PV}^{pre} = P_{j,t,PV}^{pre} \cdot \tan\varphi \end{cases} \tag{11}$$

where, φ is the power angle of the inverter. $P_{j,t,PV}^{pre}$ and $Q_{j,t,PV}^{pre}$ are the active and reactive power predicted values of DPV at node *j* at time *t*, respectively. $S_{j,PV}^{max}$ is the apparent capacity of DPV inverter at node *j*. The direction of power flowing to the distribution network is positive, that is, when the DPV absorbs reactive power, the power factor of the inverter is negative.

3.2 Short-term optimization of active power and reactive power coordination

The optimization goal of short-term optimization of active and reactive power coordination is to reduce the deviation between node voltage and reference value, reduce the cost of system network loss, and try to avoid the economic loss caused by active reduction of grid-

connected DPV. Among them, the voltage reference value is the optimized calculation result of the previous plan.

The objective function of short-term optimization model of active and reactive power coordination is:

$$\min F_{op} = F_{loss} + F_{cut} + F_{vbus} \tag{12}$$

where, F_{cut} is the penalty cost of photovoltaic active power reduction, and F_{vbus} is the artificially set voltage cost, which aims to control the voltage in the form of cost. When the voltage does not exceed the limit, its value is small, and the cost increases sharply after the voltage exceeds the limit. This paper uses the bathtub curve model function to achieve this goal [6].

The model constraints include system power flow constraints, equations (2) to (8) and DPV regulation capacity constraints, and equations (11).

3.3 Real-time control of over-limit voltage

(1) Node voltage estimation

Taking Fig. 2 as an example, it is assumed that node *n* is a voltage out-of-limit node and also a DPV node. In order to realize out-of-limit voltage control, the power-voltage relationship of the node must be analyzed in detail.

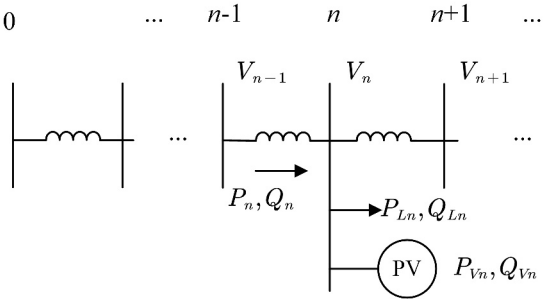

Fig. 2. Simplified feeder of distribution network.

In the figure, the total number of nodes of the line is *N*, V_0 is the terminal voltage at the head of the line, and V_n and V_{n-1} are the voltage values at node *n* and node *n-1* respectively; P_n and Q_n are the active and reactive power transmitted by the branch between node *n-1* and node *n* respectively; R_n and X_n are the resistance and reactance values of the branch respectively; P_{Vn} and $Q_{Vn}$are the active power and reactive power output by DPV at node *n*, respectively, and the direction of input power grid is positive.

According to *DistFlow* power flow algorithm [7], the relationship between node voltage and power can be simplified as follows:

$$V_{n-1}^2 = V_n^2 + 2\left(P_n R_n + Q_n X_n\right) \tag{13}$$

Assuming that the voltage at the root node of the system is constant, it is always V_0, and the voltages of node *n-1*, node *n* and node *n+1* of the system at known time *t* are respectively recorded as V_{n-1}^t, V_n^t and V_{n+1}^t. At this time, adjust the DPV injection power at node *n*, and its change values are recorded as ΔP_{Vn}^t and ΔQ_{Vn}^t, and the node load is unchanged. The expression of voltage V_n^{t+1} at node *n* at time *t+1* is as follows:

$$\left(V_n^{t+1}\right)^2 = \left(V_{n-1}^{t*}\right)^2 - \left(2\Delta P_{Vn}^t \sum_{i=1}^{n-1} R_i + 2\Delta Q_{Vn}^t \sum_{i=1}^{n-1} X_i\right) - \left(2\Delta P_{Vn}^t \sum_{i=1}^{n} R_i + 2\Delta Q_{Vn}^t \sum_{i=1}^{n} X_i\right) \tag{14}$$

(2) Active and reactive voltage regulation strategy

1) Reactive voltage regulation strategy

The core of active and reactive voltage regulation strategy in this paper is to achieve the control goal of eliminating out-of-limit voltage while avoiding unnecessary reduction of DPV active power. According to the reference [8], the relationship between the output reactive power of DPV inverter and the voltage amplitude of the junction point is put forward, and V_1 and V_4 are the upper and lower limits of system operating voltage safety. V_2 and V_3 are the voltage thresholds for the inverter to start local reactive power compensation; Q_{max} is the reactive capacity of the inverter at the current moment; If the node voltage still exceeds the limit after the reactive output at node *n* reaches Q_{max}, adjust the reactive output of other DPV nodes in the system according to the above strategy, and the inverter at node *n* keeps the reactive output at Q_{max} .

The core of regional reactive power regulation process lies in the design of reactive power regulation step size. The reactive power adjustment step size expression of other DPVs in the region is as follows:

$$\Delta Q_{pv,n+k} = 0.5\left(V_n^2 - V_4^2\right) \Big/ \sum_{i=1}^{n} X_i \tag{15}$$

$$\Delta Q_{pv,\ n-k} = 0.5\left(V_n^2 - V_4^2\right) \Big/ \sum_{i=1}^{n-k} X_i \tag{16}$$

Where, $\Delta Q_{pv,n+k}$ and $\Delta Q_{pv,n-k}$ are the upstream and downstream node adjustment step sizes *k* away from node *n*, respectively. If the reactive power capacity of all nodes in the system is exhausted, and if the voltage exceeds the limit, it will be transferred to the active power reduction and voltage regulation stage.

2) active voltage regulation strategy

At the same time, this paper considers the adjustment ability of the active and reactive power of inverter to the node voltage, and gives priority to adjusting DPV nodes with strong comprehensive adjustment ability. Considering the comprehensive voltage regulation capability of active and reactive power, the index expression of active voltage regulation capability is obtained as follows:

$$C_{j_1,n} = 2\Delta P_{Vn}^t \sum_{i=1}^{n} R_i + 2\Delta Q_{Vn}^t \sum_{i=1}^{n} X_i \tag{17}$$

$$C_{j_2,n} = 2\Delta P_{Vn}^t \sum_{i=1}^{j_2} R_i + 2\Delta Q_{Vn}^t \sum_{i=1}^{j_2} X_i \tag{18}$$

Where, $C_{j1,n}$represents the voltage regulation capability of downstream node j_1 of node *n* by active power reduction ΔP_{Vn}^t, and $C_{j2,n}$ represents the voltage regulation capability of upstream node j_2 by active power reduction ΔP_{Vn}^t.

3) Power recovery control

In the control process of reactive or active voltage regulation, when the highest voltage amplitude in the region is lower than the voltage safety limit $(V_4 + V_3)/2$, the power recovery control is started. The implementation flow of active and reactive voltage regulation strategy is shown in Fig. 3.

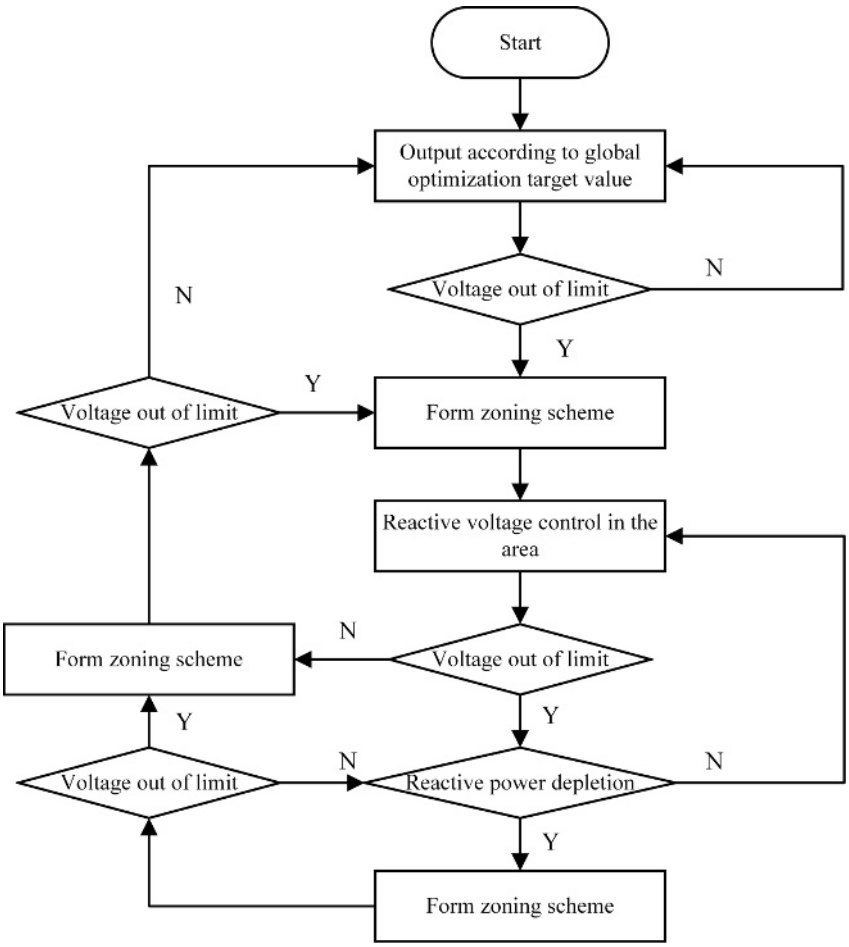

Fig. 3. Flow chart of real-time control over voltage limit.

4 Case analysis

4.1 System parameters

The structure of PG&E69 distribution system with high proportion of distributed photovoltaic is shown in Fig. 4. Node 1 is a balanced node, with the system power reference value of 10MW and the voltage reference value of 12.66kV. The total active load of the system is 3802.1kW, and the total reactive load is 2694.7kVar There are 15 DPVs in the system, of which the capacity of nodes 3, 9 and 12 is 850kW, that of nodes 17, 21, 30 and 38 is 500kW, that of nodes 41, 55 and 58 is 250kW, and that of nodes 24, 27, 60, 66 and 67 is 300kW.

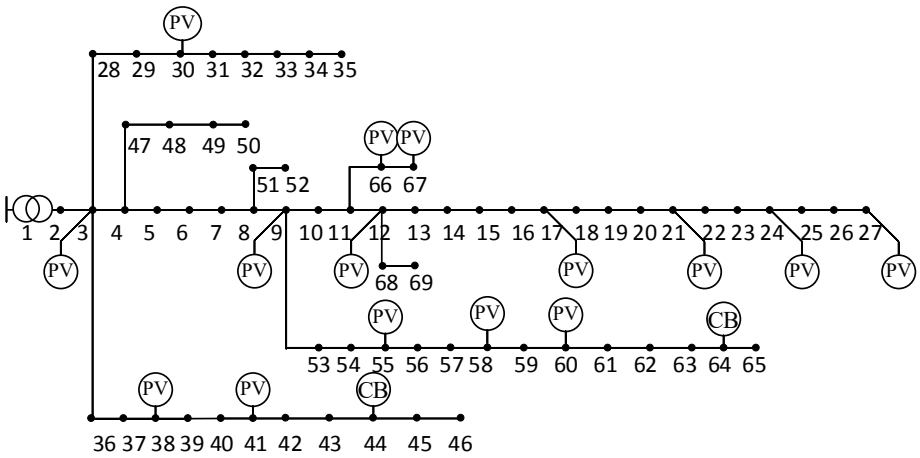

Fig. 4. PG&E69 distribution system structure diagram.

According to engineering experience, CB is incorporated into nodes 44 and 64, and OLTC is connected between nodes 1 and 2. The adjustment range of OLTC in the system is -10%~+10%, the adjustment step is 1.25%, and there are 17 gears in total. The adjustment range of CB is 0kW~900kW, the adjustment step is 150kW, and there are 6 gears in total. In a scheduling period, the upper limit of gear adjustment times of OLTC and CB devices is 10 times. The allowable deviation of node voltage in distribution network is set to -7%~+7%, and the active cost reduction coefficient of DPV is 1.5.

4.2 Analysis of results

In MATLAB 2017b, YALMIP platform calls CPLEX optimization software package to optimize the solution of the example, that is, voltage grading control is carried out on the example from three time scales, namely, plan ahead of time, short-term optimization and real-time control. The effect analysis of each level of control is as follows:

(1) Analysis of the effect of voltage reactive power plan

Fig. 5 is the curve of the forecast of system load and photovoltaic active power. Fig. 6 shows the voltage distribution of system nodes before and after the planned day at 12:00. It can be seen from the figure that before 12:00, some node voltages exceeded the upper limit, but after optimization, they no longer exceeded the limit, which proved the effectiveness of the global optimization method a few days ago. After the reactive power global optimization, the network loss cost and new gear adjustment cost are calculated, and the overall cost decreases by 13.34%, realizing the optimization of operation cost.

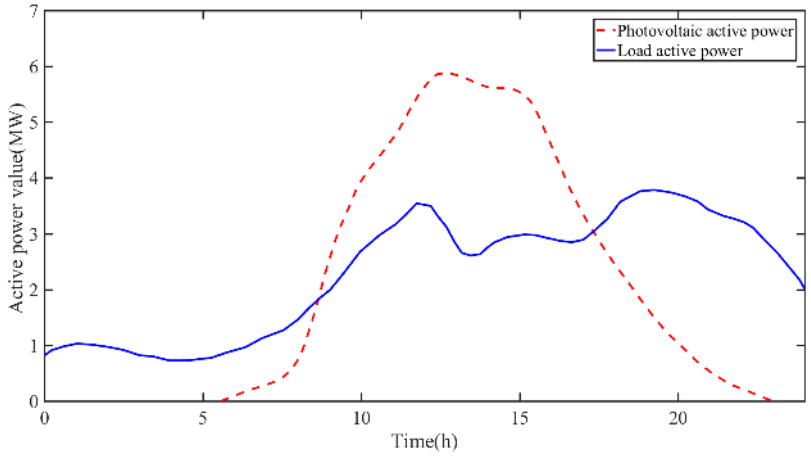

Fig. 5. System load and photovoltaic active power prediction curve.

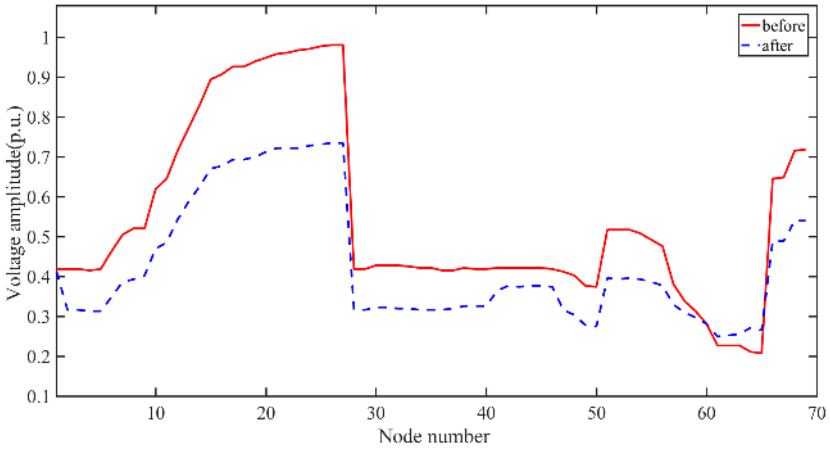

Fig. 6. Voltage distribution of the system before and after optimization at 12:00.

(2) Analysis of short-term optimization effect of active and reactive power coordination

Take the system from 12: 00 to 13: 00 as an example. At this time, the OLTC gear is -1, the CB1 gear is 6, and the CB2 gear is 5. Fig. 7 is the voltage distribution curve of the system at 12:00 before and after short-term optimization in the day.

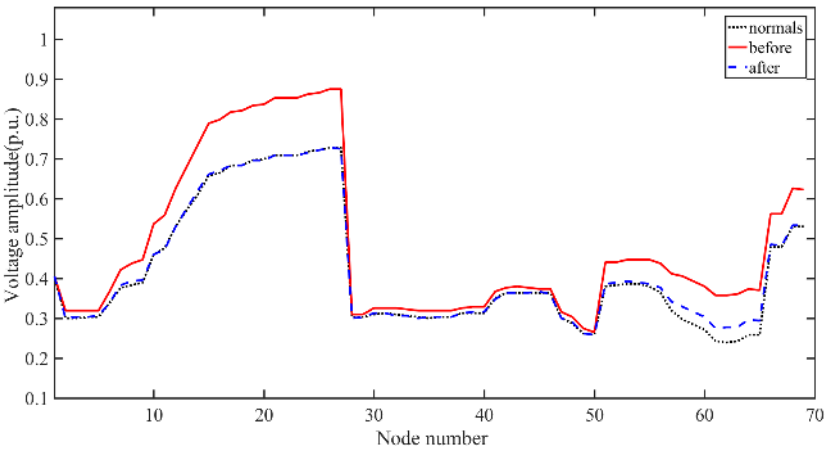

Fig. 7. Voltage distribution of the system before and after short-term optimization.

In short-time scale global optimization, the system optimizes the power flow of the system by rescheduling the active and reactive output values of DPV, so that the voltage distribution curve of the system is close to the optimization result planned recently. It can be seen from Fig. 7 that, after the short-term global optimization in the day, the voltage distribution of the system is close to the reference value set by the recent dispatch, which shows that the method in this paper can effectively reduce the risk of voltage out-of-limit caused by the forecast deviation of DPV output and load demand. By calculating the network loss cost of the system and the penalty cost caused by active reduction of DPV, the total operating cost of the optimized system is reduced by 10.99%, which shows that the short-term optimization method in this paper can optimize the operation economy of distribution network in a short time scale.

(3) Analysis of real-time control effect of over-limit voltage

Take the system at 12:00 as an example, and the system partition results are listed in Table 1. From the voltage distribution curves in Fig. 7, it can be seen that after short-term optimization of active and reactive power coordination, most of the weak points of system voltage are located in the compensation range of Area 4, so this paper introduces load disturbance to nodes in Area 4, causing the voltage of node 24 to exceed the limit, and then implements the control strategy of this paper.

Table 1. Partition result of the system at 12:00.

Area number	Photovoltaic node number	Compensation range	Number of nodes
1	3,9,30,38,41	1-9,28-53	35
2	66,67	10-11,66-67	4
3	55,58,60	54-65	12
4	12,17,21,24,27	12-27,68-69	18

Based on the current active power value of each inverter, take the adjustment step size of 10kW, and calculate the active voltage regulation capability index of each DPV node according to formula (17) and formula (18). Among them, the DPV with the strongest reactive power reduction and voltage regulation ability in the region is located at node 24, so the active power reduction and voltage regulation is obtained by multiple adjustments of the DPV at node 24.

The voltage amplitude change curve of each DPV node during voltage control is shown in Fig.8. From the data in the figure, it can be seen that by the 25th control cycle, the voltage of all nodes in the region will no longer exceed the limit, which shows that this method can effectively control the voltage exceeding the limit.

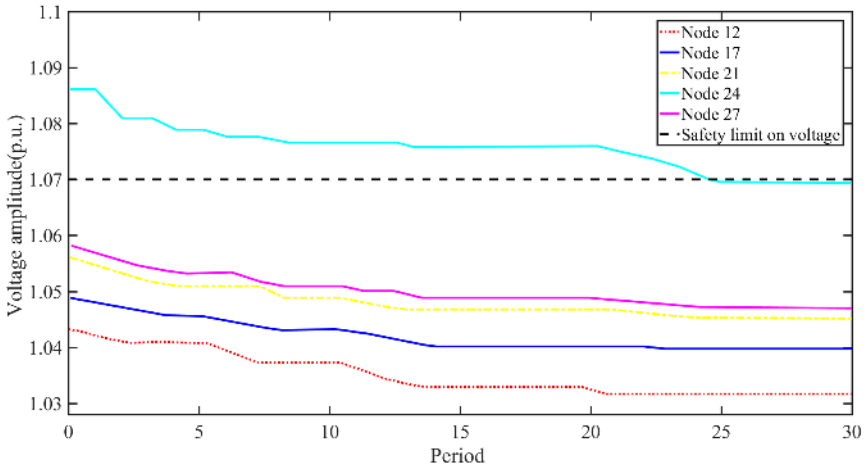

Fig. 8. Voltage change graph of DPV node in area 4.

5 Conclusion

In this paper, a voltage hierarchical control method based on multi-agent technology is proposed, which solves the voltage out-of-limit problem caused by sudden factors, and improves the operating economy and voltage safety of the system. Compared with the traditional centralized voltage control method, this method has the following characteristics:

1) Decouple the dispatching model in time through the combination of day-ahead planning and short-term optimization, and the real-time control level of over-limit voltage adopts the regional autonomy strategy to decouple the distribution network in space, thus accelerating the response speed of voltage control in distribution network.

2) Combining the characteristics of different time scales, this method designs different models and solutions for the day-ahead planning control level and the short-term optimization control level respectively, and revises the day-ahead prediction results through short-term optimization.

3) The over-limit voltage real-time control stage adopts the event triggering method, and the response of the controller under sudden disturbance is more flexible, and the control strategy of regional autonomy is conducive to quickly controlling the voltage over-limit event.

References

1. J. Schiffer, T. Seel, J. Raisch, T. Sezi, IEEE Trans. Commun **24**, 96-109(2015)
2. T. Ku, C. Lin, C. Chen, C. Hsu, W. Hsieh, S. Hsieh, IEEE Trans. Ind. Appl **52**, 1167-1174(2016)
3. C. XIAO, B. Zhao, J. Zhou, P. Li, M. Ding, Automation of Electric Power Systems **41**, 147-155(2017)
4. Y. Chai, L. Guo, C. Wang, J. Liu, L. Chang, W. Jin, J. Pan, Power System Technology **42**, 738-746(2018)

5. F. Olivier, P. Aristidou, D. Ernst, T. V. Cutsem, IEEE Trans. Smart Grid **7**, 926-936(2016)
6. X. Wang, T. Xu, C. Wang, J. Lin, J. Zhou, Proceedings of the CSEE **36**, 2918-2926(2016)
7. X. Xu, Y. Huang, C. Liu, W. Wang, Power System Technology **34**, 140-146(2010)
8. M. Bollen, A. Sannino, IEEE Trans. Power Delivery **20**, 519-520(2005)